Determination of the relative decay rate
$K_S \to \pi e\nu / K_L \to \pi e\nu$

J.R. Batley, G.E. Kalmus[1], C. Lazzeroni, D.J. Munday, M. Patel, M.W. Slater,
S.A. Wotton

Cavendish Laboratory, University of Cambridge, Cambridge, CB3 0HE, U.K.[2]

R. Arcidiacono, G. Bocquet, A. Ceccucci, D. Cundy[3], N. Doble[4], V. Falaleev,
L. Gatignon, A. Gonidec, P. Grafström, W. Kubischta, F. Marchetto[5], I. Mikulec[6],
A. Norton, B. Panzer-Steindel, P. Rubin[7], H. Wahl[8]

CERN, CH-1211 Genève 23, Switzerland

E. Goudzovski, P. Hristov[9], V. Kekelidze, L. Litov, D. Madigozhin, N. Molokanova,
Yu. Potrebenikov, S. Stoynev, A. Zinchenko

Joint Institute for Nuclear Research, Dubna, Russian Federation

E. Monnier[10], E. Swallow, R. Winston

The Enrico fermi Institute, The University of Chicago, Chicago, Illinois, 60126, U.S.A.

R. Sacco[11], A. Walker

*Department of Physics and Astronomy, University of Edinburgh, JCMB King's Buildings,
Mayfield Road, Edinburgh, EH9 3JZ, U.K.*

W. Baldini, P. Dalpiaz, P.L. Frabetti, A. Gianoli, M. Martini, F. Petrucci, M. Scarpa,
M. Savrié

Dipartimento di Fisica dell'Università e Sezione dell'INFN di Ferrara, I-44100 Ferrara, Italy

A. Bizzeti[12], M. Calvetti, G. Collazuol, G. Graziani, E. Iacopini, M. Lenti,
F. Martelli[13], G. Ruggiero, M. Veltri[13]

Dipartimento di Fisica dell'Università e Sezione dell'INFN di Firenze, I-50125 Firenze, Italy

M. Behler, K. Eppard, M. Eppard[9], A. Hirstius[9], K. Kleinknecht, U. Koch,
L. Masetti[18], P. Marouelli, U. Moosbrugger, C. Morales Morales, A. Peters[9], R. Wanke,
A. Winhart

Institut für Physik, Universität Mainz, D-55099 Mainz, Germany[14]

A. Dabrowski, T. Fonseca Martin, S. Goy Lopez, M. Velasco

*Department of Physics and Astronomy, Northwestern University, Evanston Illinois 60208-3112,
U.S.A.*

G. Anzivino, P. Cenci, E. Imbergamo, G. Lamanna, P. Lubrano, A. Michetti, A. Nappi,
M. Pepe, M.C. Petrucci, M. Piccini, M. Valdata

Dipartimento di Fisica dell'Università e Sezione dell'INFN di Perugia, I-06100 Perugia, Italy

C. Cerri, F. Costantini, R. Fantechi, L. Fiorini, S. Giudici, I. Mannelli, G. Pierazzini,
M. Sozzi

Dipartimento di Fisica, Scuola Normale Superiore e Sezione dell'INFN di Pisa, I-56100 Pisa, Italy

C. Cheshkov, J.B. Cheze, M. De Beer, P. Debu, G. Gouge, G. Marel, E. Mazzucato, B. Peyaud, B. Vallage

DSM/DAPNIA - CEA Saclay, F-91191 Gif-sur-Yvette, France

M. Holder, A. Maier, M. Ziolkowski

Fachbereich Physik, Universität Siegen, D-57068 Siegen, Germany[15]

C. Biino, N. Cartiglia, M. Clemencic, E. Menichetti, N. Pastrone

Dipartimento di Fisica Sperimentale dell'Università e Sezione dell'INFN di Torino, I-10125 Torino, Italy

W. Wislicki,

Soltan Institute for Nuclear Studies, Laboratory for High Energy Physics, PL-00-681 Warsaw, Poland[16]

H. Dibon, M. Jeitler, M. Markytan, G. Neuhofer, L. Widhalm

Österreichische Akademie der Wissenschaften, Institut für Hochenergiephysik, A-10560 Wien, Austria[17]

Abstract

The decay rate of $K_S \to \pi e \nu$ relative to the rate of $K_L \to \pi e \nu$ has been measured by the NA48 collaboration in a neutral Kaon beam originating from 400 GeV proton-Be interactions at the CERN SPS. The result is $0.993 \pm 0.026_{stat} \pm 0.022_{syst}$, compatible with 1 in agreement with the Standard Model prediction at tree level. It implies $BR(K_S \to \pi e \nu) = (7.05 \pm 0.18_{stat.} \pm 0.16_{syst.}) \times 10^{-4}$.

1   Introduction

The purpose of the present measurement is to check the prediction of the Standard Model concerning the neutral kaon semileptonic decays $\pi e \nu$ by fitting the rate of decays occurring in a neutral beam originating from hadronic interactions, as a function of the distance from the production target.

For K^0 mesons produced as strangeness eigenstates, the proper time distribution of semileptonic decays to a specific ($\pi^+ e^- \overline{\nu}$, $\pi^- e^+ \nu$) charge state can be written [1] as the sum of exponential decay terms, with the K_S and the K_L lifetimes, and K_S/K_L interference terms:

$$\left(\frac{dN}{dt}\right)_\pm = N(K^0)\left[\Gamma_{S\pm}e^{-\frac{t}{\tau_S}} + \Gamma_{L\pm}e^{-\frac{t}{\tau_L}} + I_\pm(t)\right] \tag{1}$$

$$\left(\frac{d\overline{N}}{dt}\right)_\pm = N(\overline{K}^0)\left[\overline{\Gamma}_{S\pm}e^{-\frac{t}{\tau_S}} + \overline{\Gamma}_{L\pm}e^{-\frac{t}{\tau_L}} + \overline{I}_\pm(t)\right] \tag{2}$$

If the rates to the two charge states are summed, the relative contribution of the interference terms can be neglected because their sum is of the order of the CP violation parameter $Re(\epsilon)$ and of opposite sign for initial K^0 or $\overline{K}^0$. The ratios $\frac{\Gamma_{S+}+\Gamma_{S-}}{\Gamma_{L+}+\Gamma_{L-}}$ and $\frac{\overline{\Gamma}_{S+}+\overline{\Gamma}_{S-}}{\overline{\Gamma}_{L+}+\overline{\Gamma}_{L-}}$ are equal if CPT violation is neglected. [1] Their common value

$$\frac{\Gamma_{S+} + \Gamma_{S-}}{\Gamma_{L+} + \Gamma_{L-}} = \frac{\overline{\Gamma}_{S+} + \overline{\Gamma}_{S-}}{\overline{\Gamma}_{L+} + \overline{\Gamma}_{L-}} = |\eta|^2 \tag{3}$$

is predicted to be 1 according to the standard model. In case $\Delta S = -\Delta Q$ contributions were present

$$|\eta|^2 = 1 + 4Re(x_l) \tag{4}$$

where $x_l = \Gamma(\overline{K}^0 \to \pi^- l^+ \nu)/\Gamma(K^0 \to \pi^- l^+ \nu)$.

Finally, with these approximations

$$dN/dt(\pi e \nu) \propto |\eta|^2 e^{(-t/\tau_S)} + e^{(-t/\tau_L)} \tag{5}$$

Experimentally the value of $|\eta|^2$ in the expression (5) is determined by fitting the number of predicted to the number of measured events as a function of the distance Z_v between the average position of kaon production within the target and the reconstructed decay vertex. The predicted distribution is obtained by a Monte Carlo simulation which takes into account the independently determined kaon energy production spectrum, the acceptance and the procedure of event reconstruction to translate the proper time to Z_v distribution.

---

[1] A contribution to these ratios from a non zero value of the parameter $Re(\Delta)$, describing CPT violation in kaon mixing, which appears again with opposite sign for initial K_0 and $\overline{K}_0$, is limited on the basis of a CPLEAR measurement [2] to a value smaller than our experimental sensitivity.

2   Experimental apparatus and trigger

The NA48 detector [3] was designed to measure direct CP violation in the neutral K system [4]. A K_L beam was produced at the same time as a neutral K beam originating from a target located a short distance before the beginning of the fiducial decay region. The measurement presented in this paper uses only the data taken in 2002 during a high intensity run with no K_L beam.

The experimental components relevant for this measurement include the following:

- A Be production target (40 cm long, 2 mm diameter) on which 400 GeV protons impinge at 4.2 mrad relative to the (z) axis of the neutral beam, as defined by a collimator ending 6.23 m after the center of the target.
- An 87-m long evacuated decay volume, terminated by a thin ($0.003X_0$) Kevlar window. The beam continues in a 16 cm diameter vacuum pipe throughout the following detector elements.
- Anti-counter rings veto events with photons or charged particles outside the solid angle covered by the detectors.
- A magnetic spectrometer measures the momentum of charged particles with a resolution $\sigma(p)/p = (0.48 \oplus 0.009 \times p)\%$ where p is in GeV/c. It consists of four drift chambers (DCH), each with 8 planes of sense wires along 4 directions angled 45 degrees relative to each other. The volume between the chambers is filled with helium at atmospheric pressure. The spectrometer magnet is a dipole with a field integral of 0.85 Tm placed after the first two chambers. The direction of the field was inverted several times during runs to equalize the average acceptance for particles of opposite sign. The distance between the first and last chamber is 21.8 m.
- A hodoscope of plastic scintillation counters placed downstream of the last drift chamber whose signals are used for fast pre-trigger. The offline time resolution for 2-tracks events is 200 ps.
- An electromagnetic calorimeter (LKr), a quasi-homogeneous liquid Krypton ionization chamber with 13248 longitudinal 2 cm × 2 cm read-out cells (27 X_0). The LKr energy resolution for electromagnetic showers is $\sigma(E)/E = (3.2/\sqrt{E} \oplus 9.0/E \oplus 0.42)\%$ where E is in GeV, and the shower time resolution is better than 500 ps.
- Trigger and readout systems. For this analysis only events selected by a minimum bias trigger are used. The minimum bias trigger requires at least one hit in the hodoscope in coincidence with hits in the first DCH consistent with at least two tracks. Its simplicity allows the efficiency to be as high as 99%. This trigger was downscaled and used as a control for efficiency studies of more restrictive requirements. Its use here implies a reduction of available statistics but has the advantage of allowing a straightforward simulation of acceptance as a function of the proper time of decays.

3   Event reconstruction and selection criteria

After the standard NA48 procedure reconstructing tracks in the DCH and clusters in the LKr, geometrical cuts have been applied to transverse coordinates and to time of occurrence to properly define the limits of the acceptance.

Only events with two tracks of opposite charge and one or two clusters are accepted. In addition, to select good events while rejecting backgrounds, the following criteria had to be satisfied :

- the tracks are compatible with coming from a common vertex positioned along the neutral beam within the fiducial region between 6.0 m and 50.0 m from the target center;

2

- the ratio of the track momenta is in the range 0.4-2.5;
- for the candidate electron:
  - the extrapolation of the track to the LKr matches the position of a cluster within 5 cm;
  - the ratio between the energy of this cluster and the track momentum (E/p) is between 0.95 and 1.05;
  - the energy is greater than 20 GeV;
- for the candidate pion:
  - the track is unassociated with any clusters or has $E/p < 0.8$;
  - the energy is greater than 10 GeV;
- the sum of the electron and pion energies is between 60 to 180 GeV.

The invariant mass of the two charged particles is then calculated for the mass assignments (a) πe, (b) $\pi\pi$, and (c) $p\pi$. Events are accepted only if the invariant mass:
- is less than or equal to M_K for assignment (a), and
- differs by more the 35 MeV from M_K for assignment (b), and
- differs by more than 16 MeV from M_Λ for assignment (c).

Assuming that the matrix elements for K_S and K_L decaying to $\pi e\nu$ are equal, these selection criteria do not bias the relative K_S and K_L acceptance.

Due to the missing longitudinal momentum of the undetected neutrino, a kaon decay can be assigned two different values E_1, E_2 of energy. Only events for which both E_1 and E_2 are within the range $60 \leq E \leq 180$ GeV are retained in order to reduce uncertainties in the Monte Carlo simulation. Two samples of data were taken with opposite magnetic field direction and with equal total number of events (2×204000). The Z_v distribution for the sum of these two samples is shown in Fig. 1. The shaded histograms correspond to expected K_S and K_L decay spectra obtained with the Monte Carlo procedure outlined in the following section.

4   Monte Carlo simulation

The acceptance of the apparatus has been evaluated using a GEANT based Monte Carlo simulation [5]. The geometry of the beam and detector, the active and passive properties of each component (e.g. multiple scattering, hadronic interactions, *bremsstrahlung*, photon conversion, delta rays) and the time variations of the detection efficiencies have been taken into account. Samples of $\pi e\nu$ events, of possible backgrounds and other decays of interest have been produced with adequate statistical significance. About 3×10^6 $\pi e\nu$ events were used, after reconstruction and selection.

The energy distribution of the neutral kaons produced within the beam acceptance is a critical input to the simulation. The simulated production energy of the neutral kaon has been tuned such that it reproduces the data for the reconstructed energy of $K_S \rightarrow \pi^0\pi^0$ and $K_L \rightarrow 3\pi^0$ events (see Fig. 2 and Fig. 3).

Using the same matrix element for K_S and K_L, and including radiative corrections [6], the probability that a $\pi e\nu$ decay satisfies the selection criteria and is reconstructed with an energy and vertex position within the appropriate acceptance range has been evaluated with Monte Carlo samples much larger than the data sample. This probability distribution is convoluted with the production energy spectrum and with the K_S, K_L exponential decay factors $N|\eta|^2 exp(-t/\tau_S)$ and $N exp(-t/\tau_L)$ (where N is a normalisation factor and $t = Z_v \times M_K/\sqrt{E_K^2 - c^2 M_K^2}$ is the proper time, Z_v being the reconstructed vertex and E_K being the kaon energy). Relevant kinematic distributions from the simulation are then compared with those from the experimental data. A good agreement was

found for all distributions. As an example, the distributions of visible energy in data and simulation are shown in Fig. 4.

5   Background evaluation

Background contamination of the signal at the few per mille level will not affect the significance of our determination of $|\eta|^2$.

The major source of background is the decay $K_S \to \pi^+\pi^-$, when one of the pions loses more than 95% of its energy in the LKr and the invariant mass of the pion pair is badly reconstructed, thus satisfying the semi-leptonic acceptance criteria. To evaluate the background contribution, both effects were studied in detail. The E/p distribution for pions was studied using a sample of $\pi e\nu$ candidate events selected omitting the requirement that $E/p \leq 0.8$ for one of the two tracks. As it can be derived from the data of Fig. 5, the fraction of pions with $0.95 \leq E/p \leq 1.05$, meeting the electron identification requirement, is 2.7×10^{-3}. The probability of invariant mass mis-reconstruction was studied with a simulated sample of $K_S \to \pi^+\pi^-$ events. The cut at $|m_{\pi\pi} - m_{K^0}| > 35$ MeV missed 0.25% of such events.

Contributions to the background from other K_S and K_L decays, such as $\pi\pi\gamma$ and $\pi^+\pi^-\pi^0$ or $\pi\pi$ with subsequent $\pi \to e\nu$, have been estimated to be less than one part per thousand, and therefore are neglected. The possible background from Λ decays has been rejected applying a cut on the ratio of products momenta and vetoing an interval of 3% around the Λ mass; the remaining contribution to the background is negligible.

6   Result and estimate of systematic uncertainties

To check the prediction of the Standard Model within the accuracy allowed by the statistics of the available experimental sample, the distributions of the number of events as a function of the decay vertex position Z_v, integrated over different intervals of "visible energy" $E_e + E_\pi$ were examined, since they are sensitive to $|\eta|^2$.

Because its decay length is much greater than the Z_v range, the K_L component of the distribution should be nearly flat, neglecting acceptance effects. On the other hand, the K_S contribution, which is proportional to $|\eta|^2$, decreases almost exponentially with Z_v. The relative fraction of K_S to K_L decays used to determine $|\eta|^2$ is therefore sensitive to the Z_v range used. Various ranges were used, from 750 cm to 5000 cm and increasing the minimum value in steps of 100 cm. The measurement of $|\eta|^2$ is consistent with being invariant with respect to the chosen fiducial range. The minimum value of 750 cm has been chosen to avoid effects related to the vicinity of the final collimator, ending at 623 cm.

Several other sources of systematics effects have been studied, including tests on the quality of the acceptance simulation. It was shown that the actual distribution of calorimeter dead cells has a negligible effect on this measurement. Test were done to address the effect of a difference between data and MC kaon energy distributions: variation of the minimum electron energy cut causes changes in the fit value of only about 10% of the statistical error.

The main contributions to the systematic uncertainty are:

- The uncertainty related to the average longitudinal production point in the target. Movement of the transverse position of the proton beam can produce a shift in the average position of p-Be interactions inside the target. A Monte Carlo simulation of this effect has been performed, taking into account the different attenuation lengths

4

of protons and kaons: an effective shift of ± 5 cm induces a change of $\pm 1.6\%$ in $|\eta|^2$.

   – The uncertainty in the decay form factor. Changing the coefficient λ of the q^2 term in the matrix element $(1 + \lambda q^2/m_\pi^2)$ by ± 1 standard deviation from its central value [8] results in a change of $\pm 1\%$ in $|\eta|^2$.

   – The uncertainty due to radiative corrections. The PHOTOS [6] generator and the reweighting of the events with Ginsberg [7] corrections have been used to generate extra photons; including these $|\eta|^2$ changes by $(1.0 \pm 1.0)\%$.

   – The uncertainty due to CP violation in kaon mixing. The effect of neglecting this is found to be insignificant.

The total systematic uncertainty is thus estimated to be $\pm 2.2\%$.

The final result is $|\eta|^2 = 0.993 \pm 0.026_{stat} \pm 0.022_{syst}$, which is in agreement with the Standard Model expectation at tree level of 1 . The χ^2 for the fit is $\chi^2/ndf = 80.5/83 = 0.97$.

Using the following values from [8] for $BR(K_L \to \pi e\nu = 0.4053 \pm 0.0015$, $\tau_L = (5.114 \pm 0.021) \times 10^{-8}$ s, and $\tau_S = (0.8958 \pm 0.0006) \times 10^{-10}$ s, the branching ratio for $K_S \to \pi e\nu$ is extracted: $BR(K_S \to \pi e\nu) = (7.046 \pm 0.18_{stat} \pm 0.16_{syst}) \times 10^{-4}$, in excellent agreement with the recent measurement from the KLOE collaboration of $BR(K_S \to \pi e\nu) = (7.046 \pm 0.091) \times 10^{-4}$ [9].

The above value of $|\eta|^2$ can be translated, neglecting possible CPT non invariance to a value for $Re(x_l) = (-2 \pm 10) \times 10^{-3}$. The CPLEAR experiment [10] has obtained $Re(x_l) = (-1.8 \pm 6.1) \times 10^{-3}$ and KLOE $Re(x_l) = (-0.5 \pm 3.6) \times 10^{-3}$.

A relevant feature of the present result, compared with the other quoted experiment is the fact that it is independent of any tagging procedure and is extracted from the shape of the decay length distribution, with no need of knowledge of the absolute detection efficiency.

7   ACKNOWLEDGMENTS

References

[1] see, e.g., M. Hayakawa and A. I. Sanda, Phys.Rev. **D48** (1993) 1150.

[2] A. Angelopoulos et al., Phys.Lett. **B444** (1998) 52.

[3] V. Fanti et al., Nucl. Instr. Meth., to appear.

[4] J.R. Batley et al., Phys.Lett. **B544** (2002) 97.

[5] GEANT Detector Description and Simulation Tool, CERN program Library Long Write-up W5013 (1994).

[6] E. Barberio and Z. Was, Comp. Phys. Commun. **79** (1994) 291.

[7] E. Ginsberg, Phys.Rev. **171** (1968) 1675.
E. Ginsberg, Phys.Rev. **174** (1968) 2169 erratum.
E. Ginsberg, Phys.Rev. **187** (1969) 2280 erratum.

[8] Particle Data Group, W.M. Yao et al., Journal of Physics **G33** (2006) 1.

[9] F. Ambosino et al., Phys.Lett. **B636** (2006) 173.

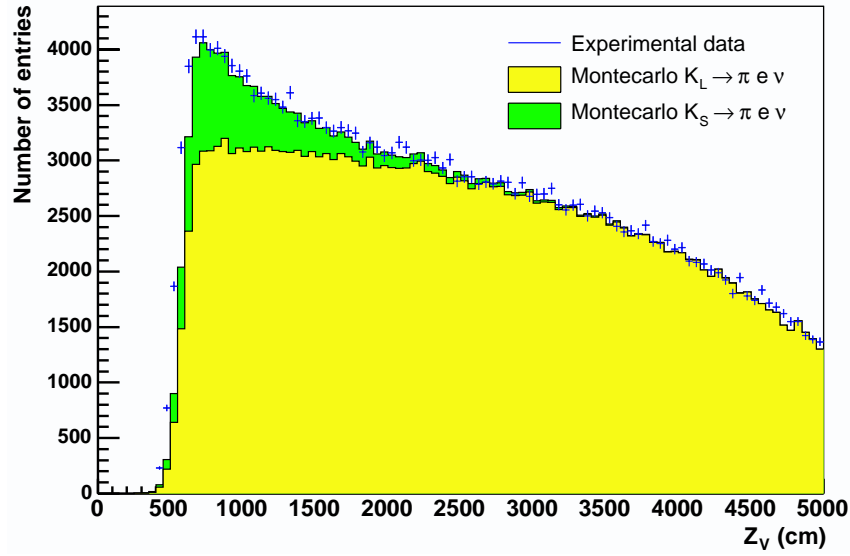[10] A. Angelopoulos et al., Phys.Lett. **B444** (1998) 38.

Figure 1: Distribution of the longitudinal coordinate of the kaon vertex, Z_v, for data selected as $K_{L,S} \to \pi e \nu$ (crosses) compared to Monte Carlo predictions (solid lines, K_L in yellow and K_S in green).
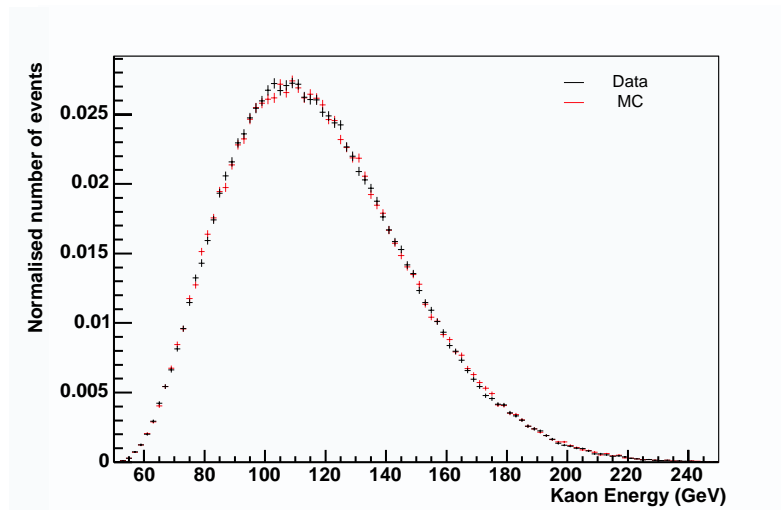

Figure 2: Kaon energy distribution for $K_S \to \pi^0 \pi^0$ events (data in black, Monte Carlo in red).

6

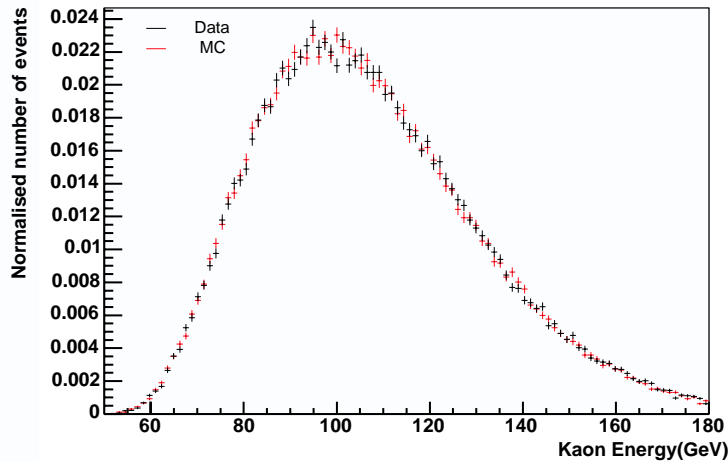Figure 3: Kaon energy distribution for $K_L \to 3\pi^0$ events (crosses represent data, while the histogram represents the Monte Carlo).
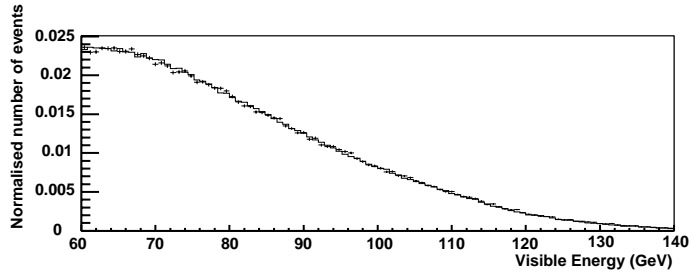

Figure 4: Kaon visible energy distribution for $K_S \to \pi e \nu$ events, for events with electron energy greater than 30 GeV (crosses represent data, while the histogram represents the Monte Carlo).
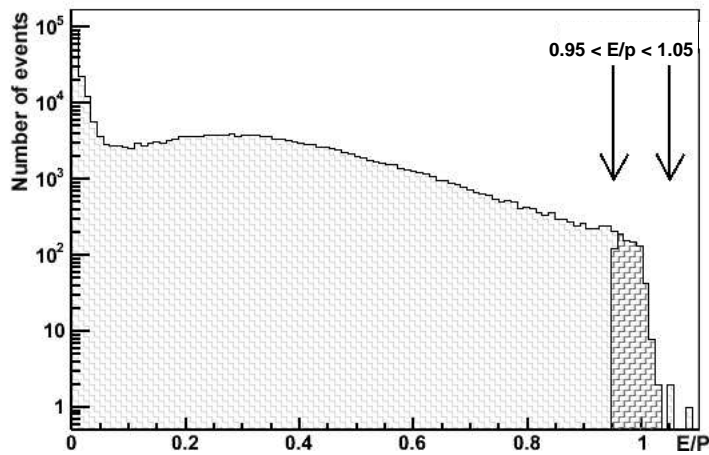

Figure 5: Pion E/p distribution for $\pi e \nu$ events; the arrows indicate the region in which the pion fakes the electron requirement.